Spectral long-range interaction of temporal incoherent solitons

Gang Xu,[1,*] Josselin Garnier,[2] and Antonio Picozzi[1]

[1]*Laboratoire Interdisciplinaire Carnot de Bourgogne (ICB), CNRS—University of Burgundy, Dijon, France*

[2]*Laboratoire de Probabilités et Modèles Aléatoires, University Paris Diderot, 75205 Paris Cedex 13, France*

**Corresponding author: gang.xu@u-bourgogne.fr*

Received November 8, 2013; accepted December 18, 2013;
posted December 23, 2013 (Doc. ID 200926); published January 27, 2014

We study the interaction of temporal incoherent solitons sustained by a highly noninstantaneous (Raman-like) nonlinear response. The incoherent solitons exhibit a nonmutual interaction, which can be either attractive or repulsive depending on their relative initial distance. The analysis reveals that incoherent solitons exhibit a long-range interaction in frequency space, which is in contrast with the expected spectral short-range interaction described by the usual approach based on the Raman-like spectral gain curve. Both phenomena of anomalous interaction and spectral long-range behavior of incoherent solitons are described in detail by a long-range Vlasov equation. © 2014 Optical Society of America

OCIS codes: (190.4370) Nonlinear optics, fibers; (190.5650) Raman effect; (030.1640) Coherence.
http://dx.doi.org/10.1364/OL.39.000590

The propagation of partially coherent nonlinear optical waves is a subject of growing interest in different fields of investigations, such as, e.g., wave propagation in homogeneous [1–5] or periodic media [6], waveguides [7], cavity systems [8–12], supercontinuum generation [13–15], shock waves [16], or nonlinear interferometry [17]. Besides the process of optical wave thermalization [5,13,14,18], incoherent solitons (IS) are known to play a natural important role in the understanding of random nonlinear waves. Originally observed experimentally in slowly responding photorefractive crystals [19], ISs have become a bloomy area of research, e.g., the modulational instability (MI) of incoherent waves [20,21], the existence of ISs with spatial or temporal nonlocal nonlinearities [22–25], or spectral incoherent solitons in optical fibers [26,27]. A notable progress in the study of incoherent optical waves has been also accomplished by exploiting analogies with nonlinear plasma phenomena [2,4,21,24,25,28].

In this Letter we revisit the problem of propagation of temporally incoherent waves in a Kerr medium characterized by a noninstantaneous response time. As a result of the causality property inherent to the nonlinear response function, $R(t)$, the spectral dynamics of an incoherent wave is usually described by the Raman-like spectral gain curve, $g(\omega) = \Im[\tilde{R}(\omega)]$, which is defined as the imaginary part of the Fourier transform of $R(t)$. The typical bandwidth of $g(\omega)$, say $\Delta\omega_g \sim 1/\tau_R$, denotes the characteristic interaction range in frequency space, where τ_R denotes the response time of the nonlinearity.

We show here that the spectral dynamics of incoherent waves is no longer captured by the spectral gain function $g(\omega)$ when one considers a *highly* noninstantaneous response of the nonlinearity. Indeed, a long-range interaction in the temporal domain, $\tau_R \gg \tau_0$, τ_0 being the characteristic ("healing") time [4], should lead to a short-range interaction in frequency space, $\Delta\omega_g \sim 1/\tau_R \ll 1/\tau_0$. Conversely, *we show that a long-range interaction in the time domain implies a long-range interaction in the spectral domain*, i.e., an interaction whose spectral range is of order $\Delta\omega_{\rm int} \sim 1/\tau_0 \gg \Delta\omega_g$.

We illustrate this spectral long-range behavior by considering the interaction of two temporal ISs, whose existence is known to require a highly noninstantaneous nonlinearity [25]. The analysis reveals that, despite its phase-insensitive character [29,30], the interaction of ISs can be either attractive or repulsive, depending on their relative initial distance. Both phenomena of anomalous interaction and spectral long-range behavior are described in detail by a long-range Vlasov formulation [4], which differs from the traditional Vlasov equations considered to study incoherent MI and ISs in plasmas [31], hydrodynamics [32], and optics [2,27,28]. We envisage the experimental observation of this spectral long-range interaction of ISs owing to the recent progress made on the fabrication of photonic crystal fibers filled with liquids displaying highly noninstantaneous Kerr responses [33].

We consider the standard nonlinear Schrödinger (NLS) equation accounting for a noninstantaneous nonlinear response function

$$i\partial_z\psi + s\partial_{tt}\psi + \sigma\psi\int R(t-t')|\psi|^2(z,t')\mathrm{d}t' = 0. \quad (1)$$

For convenience, we normalized the equation with respect to the "healing time" $\tau_0 = \sqrt{|\beta|/(|\gamma|\rho)}$ and the length scale $L_0 = 1/(|\gamma|\rho)$, where ρ is the power, β the dispersion coefficient [$s = \mathrm{sign}(\beta)$], and γ the nonlinear coefficient [$\sigma = \mathrm{sign}(\gamma)$]. The time τ_0 plays a key role: it refers to the time scale for which linear and nonlinear effects are of same order of magnitude, e.g., τ_0 is the typical MI period in the limit of an instantaneous nonlinearity [4]. The variables can be recovered in real units through the transformations $t \to t\tau_0$, $z \to zL_0$, $\psi \to \psi\sqrt{\rho}$ and $R(t) \to \tau_0 R(t)$. Hence, $\mathcal{N}/T_0 = T_0^{-1}\int|\psi|^2\mathrm{d}t = 1$, where T_0 is the temporal numerical window. We use the convention that $t > 0$ corresponds to the leading edge of the pulse [$R(t) = H(-t)\bar{R}(-t)$, $H(t)$ being the Heaviside function], so that the causal response will be on the trailing edge of a pulse, i.e., $R(t) = 0$ for $t > 0$.

We consider the IS regime discussed in [25], i.e., the focusing regime with normal dispersion, $s=-1$, $\sigma=+1$ (which is formally equivalent to the defocusing regime with anomalous dispersion, $s=+1, \sigma=-1$). These temporal ISs are of a fundamentally different nature than usual spatial bright solitons, which require $s\sigma=+1$ (for details, see [25]). We report in Figs. 1,2 the evolution of two ISs that has been obtained by integrating numerically the NLS Eq. (1). We considered in this example a long-range Gaussian-like response, $\bar{R}(t)=t^2\exp[-t^2/(2\tau_R^2)]/(\tau_R^3\sqrt{\pi/2})$, with $\tau_R=200$. Note that the Raman-like response function will be discussed later. The simulations reveal that the ISs exhibit an anomalous interaction, which can be either attractive or repulsive depending on their relative initial distance, as illustrated in Fig. 2. Contrarily to spatial IS interactions [29,30], here, the IS interaction is phase-insensitive. Note that this may be interpreted in analogy with the phase-insensitive interaction of ISs in instantaneous nonlocal media [22], since a nonlocal instantaneous nonlinearity exhibits properties analogous to the local noninstantaneous nonlinearity considered here. The attractive IS interaction in Fig. 1 is characterized by a spiralling dynamics in the spectrogram, which eventually leads to a coalescence of the ISs into a single soliton. Besides the constant acceleration of ISs discussed in detail in [25], the spiralling behavior unveils the existence of a long-range interaction in both the temporal and spectral domains. In dimensional units, the spectral separation between the ISs is of order $\Delta\omega_{\rm int}\sim 1/\tau_0 \gg \Delta\omega_g\sim 1/\tau_R$: in the example of Fig. 1 $\Delta\omega_{\rm int}/\Delta\omega_g\sim\tau_R/\tau_0=200$. This is in marked contrast with usual coherent Raman soliton interactions, in which $\Delta\omega_{\rm int}$ is of the same order as $\Delta\omega_g$ (see e.g. [34,35]).

This anomalous IS interaction can be described by the long-range Vlasov equation [4,25]. It governs the evolution of the averaged spectrum of the wave, $n_\omega(t,z)=\int B(t,\tau,z)\exp(i\omega\tau)\mathrm{d}\tau$, where $B(t,\tau,z)=\langle\psi(t-\tau/2,z)\psi^*(t+\tau/2,z)\rangle$ is the auto-correlation function

$$\partial_z n_\omega(t,z)=2\omega\partial_t n_\omega(t,z)-\partial_t U(t,z)\partial_\omega n_\omega(t,z), \quad (2)$$

where $N(t,z)=(2\pi)^{-1}\int n_\omega(t,z)\mathrm{d}\omega$ is the averaged intensity of the incoherent wave, and $U(t,z)=R*N$ the self-consistent potential, $*$ denoting the temporal convolution product (we remind that $s=-1$, $\sigma=1$). Equation (2) conserves $\mathcal{N}=\int N(t,z)\mathrm{d}t$. Contrary to the spatial case [4], in the temporal domain the potential $U(t,z)$ is constrained by the causality of $R(t)$, which breaks the Hamiltonian structure of the Vlasov Eq. (2). Then the total momentum, $\mathcal{P}(z)=(2\pi)^{-1}\iint\omega n_\omega(t,z)\mathrm{d}t\mathrm{d}\omega$, is no longer conserved and evolves according to $\partial_z\mathcal{P}(z)=-\int U(t,z)\partial_t N(t,z)\mathrm{d}t$. The position of the wave-packet in the time domain, $\mathcal{T}(z)=(2\pi)^{-1}\iint t n_\omega(t,z)\mathrm{d}t\mathrm{d}\omega$, verifies $\partial_z\mathcal{T}(z)=-2\mathcal{P}(z)$. Hence, the spectral and temporal positions of an IS are closely related: because of group-velocity dispersion, the linear spectral red-shift of the IS, $\mathcal{P}(z)=-\mathcal{N}\alpha z$, entails a constant acceleration of the IS, $\mathcal{T}(z)=\mathcal{T}(0)+\alpha\mathcal{N}z^2$ (see Figs. 1,2).

The spectral long-range behavior of ISs can be interpreted through a qualitative analysis of the Vlasov equation. Let us denote by $\Delta\omega_{\rm int}$ and $\Delta t\sim\tau_R$ the typical spectral and temporal widths of an incoherent wave-packet, e.g., an IS. We consider a typical evolution in which linear and nonlinear effects [i.e., second and third terms in Eq. (2)] are of the same order of magnitude: $2\omega\partial_t n_\omega(t,z)\sim\partial_t U\partial_\omega n_\omega(t,z)$, or $\Delta\omega_{\rm int}^2\sim U=R*N$. To qualitatively assess the potential U, it proves convenient to rescale the functions by introducing the small parameter $\varepsilon=1/\tau_R\ll 1$, $R(t)=\varepsilon R_0(\varepsilon t)$, and $N(t,z)=T_0\varepsilon N_0(\varepsilon t,\varepsilon z)$, where T_0 scales as $\sim 1/\varepsilon$. One obtains $U(t,z)=T_0\varepsilon U_0(T,Z)$, with $U_0(T,Z)=R_0*N_0$, $T=\varepsilon t$, and $Z=\varepsilon z$. Since $\int N_0(T,Z)\mathrm{d}T=1$ and $\int R_0(T)\mathrm{d}T=1$, the typical amplitudes and widths of $R_0(T)$ and $N_0(T,Z)$ are now of order one, which thus readily gives $\Delta\omega_{\rm int}^2\sim U_0\sim 1$. In dimensional units this result reads $\Delta\omega_{\rm int}\sim 1/\tau_0\gg 1/\tau_R$, which gives $\Delta\omega_{\rm int}/\Delta\omega_g\sim\tau_R/\tau_0$:

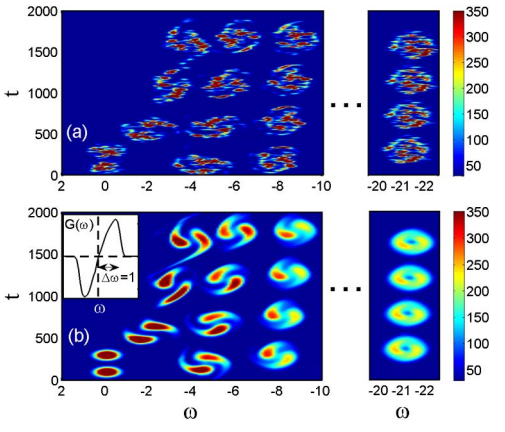

Fig. 1. Simulations of the NLS Eq. (1) (a) and Vlasov Eq. (2) (b), showing the attractive interaction between two ISs, whose initial distance is $\tau_d=\tau_R$. The ISs spiral around each other and eventually fuse into a single IS. From left to right $z=0$, 190, 300, 380; 450, 500, 550, 600; 790, 820, 850, 880; 2140, 2150, 2160, 2170 ($T_0=2048$). A quantitative agreement is obtained between NLS and Vlasov simulations, without adjustable parameters. The inset shows the antisymmetric spectral deformation, $G(\omega,z_0)=\partial_z S(\omega)$ (reminiscent of a "gain spectrum"), with a spectral long-range bandwidth $\Delta\omega_{\rm int}\sim 1$ ($z_0=2170$).

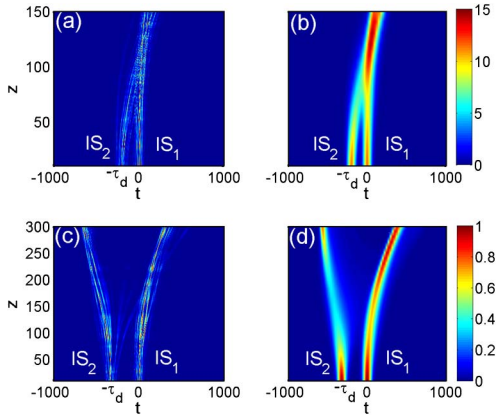

Fig. 2. Evolutions of the intensities $N_{1,2}(t,z)$ versus z showing the attractive [1st row: $\tau_d=\tau_R$, (a) NLS, (b) Vlasov] and the repulsive [2nd row: $\tau_d=1.6\tau_R$, (c) NLS, (d) Vlasov] interaction of a pair of ISs ($T_0=2048$).

the typical spectral width of an IS is τ_R/τ_0 larger than the spectral width of the gain curve $g(\omega)$. Note that this reasoning does not involve the spectral gain function $g(\omega)$, so that the spectral long-range interaction appears as a property inherent to the long-range Vlasov formalism. This spectral long-range behavior ($\Delta\omega \sim 1$) is illustrated in the inset of Fig. 1(b) through the antisymmetric spectral deformation $G(\omega) = \partial_z S(\omega) = -\int \partial_t U \partial_\omega n_\omega(t)\mathrm{d}t$, where $S(\omega) = \int n_\omega(t)\mathrm{d}t$ is the wave spectrum.

As discussed in [25], the spectral-shift of an IS, with spectral velocity α, leads to a constant acceleration of the IS. It thus proves convenient to study the interaction of a pair of (sufficiently separated) ISs in their own accelerating reference frame, $\xi = z$, $\tau = t - \alpha z^2$, $\Omega = \omega + \alpha z$, in which the coupled Vlasov equations for $n_j(\Omega, \tau, \xi)(j = 1, 2)$ read

$$\partial_\xi n_j = 2\Omega \partial_\tau n_j - \partial_\tau \tilde{U}(\tau, \xi)\partial_\Omega n_j. \tag{3}$$

The ISs are coupled by the self-consistent potential, which results from the noninertial nature of the reference frame $\tilde{U}(\tau, \xi) = U_1(\tau, \xi) + U_2(\tau, \xi) + \alpha\tau$, where $U_j(\tau, \xi) = R * N_j$ and $N_j(\tau, \xi) = (2\pi)^{-1}\int n_j(\Omega, \tau, \xi)\mathrm{d}\Omega$. As discussed in [25], the linear term in the potential, $\alpha\tau$, finds its origin in the fictitious force due to the noninertial nature of the reference frame.

In the following we study the interaction of two ISs through the analysis of their spectral and temporal dynamics in the noninertial reference frame, i.e., $\mathcal{P}_j(\xi) = (2\pi)^{-1}\iint \Omega n_j(\Omega, \tau, \xi)\mathrm{d}\tau\mathrm{d}\Omega$ and $\mathcal{T}_j(\xi) = (2\pi)^{-1}\iint \tau n_j(\Omega, \tau, \xi)\mathrm{d}\tau\mathrm{d}\Omega$. Using Eq. (3), we obtain

$$\frac{1}{2}\partial_\xi^2 \mathcal{T}_j(\xi) = -\partial_\xi \mathcal{P}_j(\xi) = \mathcal{S}_j(\xi) + \mathcal{X}_j(\xi), \tag{4}$$

where $\mathcal{S}_j = -\int \partial_\tau \tilde{U}_j(\tau, \xi)N_j(\tau, \xi)\mathrm{d}\tau$ denotes the self-interaction of the j-th IS (IS_j), while $\mathcal{X}_j = -\int \partial_\tau U_{3-j}(\tau, \xi)N_j(\tau, \xi)\mathrm{d}\tau$ describes the cross-interaction between them, with $\tilde{U}_j(\tau, \xi) = U_j(\tau, \xi) + \alpha\tau$. We consider the interaction of two ISs of the same power $\mathcal{N}_1 = \mathcal{N}_2 = \mathcal{N}/2$, the first one being located at $\tau = 0$, the second one at $\tau = -\tau_d < 0$ (see Figs. 2–4). We treat the interaction among the ISs as a perturbation, so as to write $N_j(\tau, \xi) = N_j^s(\tau) + \delta N_j(\tau, \xi)$ with $|\delta N_j|(\tau, \xi) \ll N_j^s(\tau)$, while $N_j^s(\tau)$ denotes the IS temporal profile, which is stationary (ξ-invariant) in its own accelerating reference frame. We have $U_j(\tau, \xi) = U_j^s(\tau) + \delta U_j(\tau, \xi)$, where $U_j^s(\tau) = R * N_j^s(\tau)$ and $\delta U_j(\tau, \xi) = R * \delta N_j(\tau, \xi)$. In this way, $\tilde{U}_j^s(\tau) = U_j^s(\tau) + \alpha\tau$ denotes the self-consistent potential of a single IS, whose spectral velocity is determined by the condition that $\tilde{U}_j^s(\tau)$ has a minimum at the IS position [25], i.e., $\alpha = -\partial_\tau U_1^s|_{\tau=0} = -\partial_\tau U_2^s|_{\tau=-\tau_d}$. At first-order, Eq. (4) then reads $(1/2)\partial_\xi^2 \mathcal{T}_j(\xi) = -\partial_\xi \mathcal{P}_j(\xi) = -\int \partial_\tau \tilde{U}_j^s(\tau)N_j^s(\tau)\mathrm{d}\tau - \int \partial_\tau U_{3-j}^s(\tau)N_j^s(\tau)\mathrm{d}\tau$. The first term vanishes because a single IS does not exhibit spectral shift in its own reference frame. Then we obtain

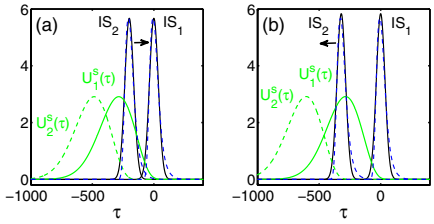

Fig. 3. Gaussian intensity profiles $N_j^s(\tau)$ (black) and corresponding potentials $U_2^s(\tau)$ (dashed-green), $U_1^s(\tau)$ (green) for $\tau_d = \tau_R$ (a) and $\tau_d = 1.6\tau_R$ (b). The dashed blue lines correspond to the IS solutions obtained from Vlasov simulations [Eq. (2)]. The arrows indicate the "particle motions" of IS_2 in $U_1^s(\tau)$. [For visibility reasons, we plotted $N_j^s(\tau)/2$].

$$\frac{1}{2}\partial_\xi^2 \mathcal{T}_j(\xi) = -\partial_\xi \mathcal{P}_j(\xi) = -\int \partial_\tau U_{3-j}^s(\tau)N_j^s(\tau)\mathrm{d}\tau \tag{5}$$

to leading order in the perturbation amplitude. As illustrated in Fig. 3, Eq. (5) explicitly reveals the nonmutual character of IS interaction: IS_1 affects the evolution of IS_2, while IS_2 leaves unaffected the evolution of IS_1. Indeed, because of the causality condition, we have $(1/2)\partial_\xi^2 \mathcal{T}_1 = -\partial_\xi \mathcal{P}_1 = -\int \partial_\tau U_2^s(\tau)N_1^s(\tau)\mathrm{d}\tau \simeq 0$, whereas $(1/2)\partial_\xi^2 \mathcal{T}_2 = -\partial_\xi \mathcal{P}_2 = -\int \partial_\tau U_1^s(\tau)N_2^s(\tau)\mathrm{d}\tau \neq 0$ whenever τ_d is smaller than or of the same order as τ_R. The nonmutual IS interaction is also apparent in the spectral dynamics through nonconservation of the total momentum, $\partial_\xi \mathcal{P}_1 + \partial_\xi \mathcal{P}_2 \neq 0$. Expanding the potential as $\partial_\tau U_1^s(\tau) \simeq \partial_\tau U_1^s|_{\tau=-\tau_d} + (\tau + \tau_d)\partial_\tau^2 U_1^s|_{\tau=-\tau_d}$, we get

$$\frac{1}{2}\partial_\xi^2 \mathcal{T}_2(\xi) = -\partial_\xi \mathcal{P}_2(\xi) \simeq -\frac{\mathcal{N}}{2}\partial_\tau U_1^s|_{\tau=-\tau_d}. \tag{6}$$

This reveals the existence of a threshold distance (τ_{th}) between the ISs defined by $\partial_\tau U_1^s|_{\tau=-\tau_{\mathrm{th}}} = 0$: for $\tau_d < \tau_{\mathrm{th}}$ ($\tau_d > \tau_{\mathrm{th}}$), we have $\partial_\tau U_1^s|_{\tau=-\tau_d} < 0$ ($\partial_\tau U_1^s|_{\tau=-\tau_d} > 0$), so that IS_2 is attracted to (repulsed from) IS_1, while this latter remains unaffected by the presence of IS_2 (see Fig. 3). A good agreement has been obtained between

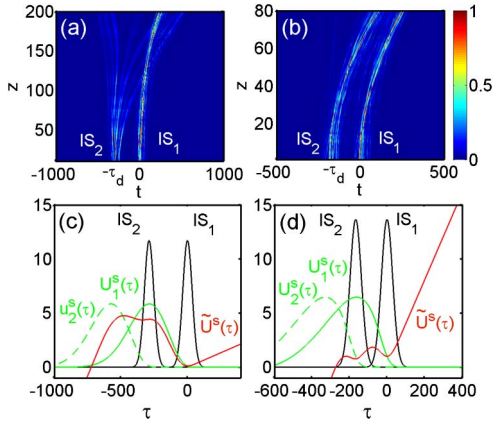

Fig. 4. (a) and (b) Evolutions of the temporal intensity profiles $N_j(t, z)$ versus z for two ISs initially separated by the threshold distance, $\tau_d = \tau_{\mathrm{th}}$, for the Gaussian-like response ($\tau_{\mathrm{th}} \simeq 1.435\tau_R$, first column) and Raman-like response ($\tau_{\mathrm{th}} \simeq 0.831\tau_R$, second column). (c) and (d) IS_j profiles $N_j^s(\tau)$ and potentials $U_j^s(\tau)$, $\tilde{U}^s(\tau)$ ($T_0 = 4096$, for visibility reasons we plotted $N_j^s(\tau)/2$).

criterion (6) and the numerical simulations of the Vlasov and NLS Eqs. (1,2), with both the Gaussian-like response and the Raman-like response, $\bar{R}(t) = (1 + \eta^2/\eta\tau_R)\sin(\eta t)\exp(-t/\tau_R)$.

The IS interaction for $\tau_d \simeq \tau_{\text{th}}$ crucially depends on the response function $\bar{R}(t)$ (see Fig. 4). For the Gaussian-like response, IS_2 exhibits a splitting in which nearly half of power ($\mathcal{N}_2/2$) is attracted to IS_1, the other is repulsed. Conversely, for the Raman-like response, IS_2 preserves its soliton shape during the propagation, with a nearly constant distance to IS_1, as described by (6) [$\mathcal{T}_2(\xi) = \mathcal{T}_2(0)$ for $\tau_d = \tau_{\text{th}}$]. Note however that such different behaviors cannot be captured by $\mathcal{T}_2(\xi)$. The robust self-trapping of IS_2 is explained by the potential in the accelerated reference frame, $\tilde{U}^s(\tau) = U_1^s(\tau) + U_2^s(\tau) + \alpha\tau$: contrary to the Gaussian-like response, for the Raman-like response IS_2 gets trapped by its self-induced potential during the propagation (Fig. 4d, red line).

We have reported an anomalous attractive-repulsive interaction of temporal ISs. The Vlasov formalism reveals that these ISs are characterized by a spectral long-range interaction, with a spectral range τ_R/τ_0 larger than the expected Raman-like spectral gain bandwidth.

This work has been supported by the Labex ACTION program (contract ANR-11-LABX-01-01). Gang Xu thanks Jiaer Zhang and Massimiliano Guasoni for the support.

References

1. A. Piskarskas, V. Pyragaite, and A. Stabinis, Phys. Rev. A **82**, 053817 (2010).
2. D. Dylov and J. Fleischer, in *Localized States in Physics: Solitons and Patterns*, Part 1, (Springer, 2011), pp. 17–34.
3. A. Picozzi and M. Haelterman, Phys. Rev. Lett. **92**, 103901 (2004).
4. J. Garnier, M. Lisak, and A. Picozzi, J. Opt. Soc. Am. B **29**, 2229 (2012).
5. J. Laurie, U. Bortolozzo, S. Nazarenko, and S. Residori, Phys. Rep. **514**, 121 (2012).
6. Y. Silberberg, Y. Lahini, Y. Bromberg, E. Small, and R. Morandotti, Phys. Rev. Lett. **102**, 233904 (2009).
7. P. Aschieri, J. Garnier, C. Michel, V. Doya, and A. Picozzi, Phys. Rev. A **83**, 033838 (2011).
8. C. Conti, M. Leonetti, A. Fratalocchi, L. Angelani, and G. Ruocco, Phys. Rev. Lett. **101**, 143901 (2008).
9. S. Babin, D. Churkin, A. Ismagulov, S. Kablukov, and E. Podivilov, J. Opt. Soc. Am. B **24**, 1729 (2007).
10. E. Turitsyna, S. Smirnov, S. Sugavanam, N. Tarasov, X. Shu, S. Babin, E. Podivilov, D. Churkin, G. Falkovich, and S. Turitsyn, Nat. Photonics **7**, 783 (2013).
11. R. Weill, B. Fischer, and O. Gat, Phys. Rev. Lett. **104**, 173901 (2010).
12. A. Schwache and F. Mitschke, Phys. Rev. E **55**, 7720 (1997).
13. B. Barviau, B. Kibler, and A. Picozzi, Phys. Rev. A **79**, 063840 (2009).
14. B. Barviau, J. Garnier, G. Xu, B. Kibler, G. Millot, and A. Picozzi, Phys. Rev. A **87**, 035803 (2013).
15. M. Erkintalo, M. Surakka, J. Turunen, A. T. Friberg, and G. Genty, Opt. Lett. **37**, 169 (2012).
16. J. Garnier, G. Xu, S. Trillo, and A. Picozzi, Phys. Rev. Lett. **111**, 113902 (2013).
17. S. Derevyanko and E. Small, Phys. Rev. A **85**, 053816 (2012).
18. P. Suret, S. Randoux, H. R. Jauslin, and A. Picozzi, Phys. Rev. Lett. **104**, 054101 (2010).
19. M. Mitchell, Z. Chen, M. Shih, and M. Segev, Phys. Rev. Lett. **77**, 490 (1996).
20. M. Soljacic, M. Segev, T. Coskun, D. N. Christodoulides, and A. Vishwanath, Phys. Rev. Lett. **84**, 467 (2000).
21. B. Kibler, C. Michel, J. Garnier, and A. Picozzi, Opt. Lett. **37**, 2472 (2012).
22. C. Rotschild, T. Schwartz, O. Cohen, and M. Segev, Nat. Photonics **2**, 371 (2008).
23. W. Królikowski, O. Bang, and J. Wyller, Phys. Rev. E **70**, 036617 (2004).
24. A. Picozzi and J. Garnier, Phys. Rev. Lett. **107**, 233901 (2011).
25. C. Michel, B. Kibler, J. Garnier, and A. Picozzi, Phys. Rev. A **86**, 041801(R) (2012).
26. A. Picozzi, S. Pitois, and G. Millot, Phys. Rev. Lett. **101**, 093901 (2008).
27. J. Garnier and A. Picozzi, Phys. Rev. A **81**, 033831 (2010).
28. B. Hall, M. Lisak, D. Anderson, R. Fedele, and V. E. Semenov, Phys. Rev. E **65**, 035602 (2002).
29. T.-S. Ku, M.-F. Shih, A. A. Sukhorukov, and Y. S. Kivshar, Phys. Rev. Lett. **94**, 063904 (2005).
30. D. Anderson, L. Helczynski-Wolf, M. Lisak, and V. E. Semenov, Opt. Commun. **281**, 3919 (2008).
31. A. Hasegawa, Phys. Fluids **18**, 77 (1975).
32. M. Onorato, A. Osborne, R. Fedele, and M. Serio, Phys. Rev. E **67**, 046305 (2003).
33. C. Conti, M. Schmidt, P. Russell, and F. Biancalana, Phys. Rev. Lett. **105**, 263902 (2010).
34. F. Luan, D. V. Skryabin, A. V. Yulin, and J. C. Knight, Opt. Express **14**, 9844 (2006).
35. A. Hause and F. Mitschke, Phys. Rev. A **80**, 063824 (2009).